Blocking of STAT3 activation by miR-491, acting via EGFR, is involved in metastasis of hepatocellular carcinoma cells through inhibiting cancer stem cell-like properties

Yang Liu[1,*], Yawei Liu[2,3,*], Fei Luo[4,5], Feng Liu[1], Litian Hu[2], Yi Liu[4,5], Jianping Zhang[2], Qizhan Liu[4,5] and Weimin Fan[1]

[1]Department of Orthopedics, The First Affiliated Hospital, Nanjing Medical University, Nanjing 210029, Jiangsu, People's Republic of China

[2]Department of General Surgery, The Second Affiliated Hospital, Nanjing Medical University, Nanjing 210011, Jiangsu, People's Republic of China

[3]Department of General Surgery, Nanjing Drum Tower Hospital, Nanjing University Medical School, Nanjing 210008, Jiangsu, People's Republic of China

[4]Institute of Toxicology, School of Public Health, Nanjing Medical University, Nanjing 211166, Jiangsu, People's Republic of China

[5]The Key Laboratory of Modern Toxicology, Ministry of Education, School of Public Health, Nanjing Medical University, Nanjing 211166, Jiangsu, People's Republic of China

[*]These authors have contributed equally to this work

Correspondence to: *Qizhan Liu,* ***email:*** *qzliu@njmu.edu.cn*
Weimin Fan, ***email:*** *fanweimin@vip.sina.com*

Keywords: *hepatocellular carcinoma, miR-491, cancer stem cell-like properties, migration*

Received: *June 29, 2017* ***Accepted:*** *August 04, 2017* ***Published:*** *September 23, 2017*

ABSTRACT

Hepatocellular carcinoma (HCC) is the third leading cause of cancer-related mortality worldwide. However, the mechanisms that contribute to tumor metastasis remain unclear. To determine the molecular mechanisms underlying the metastasis of HCC cells, HepG2 (very low migratory capacity), MHCC97L (low migratory capacity), and MHCC97H (high migratory capacity) cells, as well as HCC tissues and corresponding non-cancerous liver tissue were used to investigate the effects of microRNA-491 (miR-491) on the acquisition of cancer stem cell (CSC)-like properties, neoplastic capacity, and migration of HCC cells. In HCC specimens, miR-491 levels were down-regulated, EGFR levels were up-regulated, and STAT3 was activated, results that correlated with the clinical stage of HCC. Moreover, miR-491 levels inversely correlated with the migratory potential of HCC cell lines. In HepG2 cells, down-regulation of miR-491 levels increased the levels of EGFR and STAT3 phosphorylation. In contrast, an miR-491 mimic induced contrary changes in MHCC97H cells. In HCC cells, miR-491 inhibited the luciferase activities of an EGFR 3'UTR Luc construct, indicating that miR-491 directly regulates EGFR. The effects of miR-491 on the activation were blocked by EGFR siRNA or the pEGFP-EGFR plasmid. In HepG2 cells, down-regulation of miR-491 increased the levels of CSC-like markers (Bmi-1, Oct-4, CD133, and EPCAM) and the levels of metastasis markers (MMP-9 and MMP-2) and enhanced the acquisition of CSC-like properties, neoplastic capacity, and migration; these effects were blocked by STAT3 siRNA. In contrast, over-expression of miR-491 decreased the levels of Bmi-1, Oct-4, CD133, EPCAM, MMP-9, and MMP-2 and inhibited the acquisition of CSC-like properties, neoplastic capacity, and migration of MHCC97H cells; the effects

were blocked by up-regulation of STAT3 levels. These results indicate that miR-491 influences CSC-like properties and metastasis of HCC cells by blocking the activation of STAT3 via EGFR, which provides a mechanism for preventing metastasis of HCCs.

INTRODUCTION

Hepatocellular carcinoma (HCC), a highly malignant human cancer, is the third greatest cause of cancer-related death globally [1], and more than a half of new cases and deaths occur in China [2]. The treatments of HCC include surgical resection, liver transplantation, radio immunotherapy, and chemotherapy. The choice of treatment depends on the cancer stage, resource availability, and practitioner choices [3]. In spite of advances in HCC diagnosis and treatment, there have been few noteworthy improvements in overall survival; the 5-year survival rate after surgical resection remains below 30% due to the high rate of recurrence [4].

MicroRNAs (miRNAs) are non-coding RNAs that interact with the 3′-untranslated regions (3′-UTRs) of the target mRNAs and inhibit gene expression by blocking their translation or by degrading them [5, 6]. miRNAs participate in many biological processes, including development, differentiation, apoptosis, and proliferation [7]. They also regulate the expression of oncogenes and tumor suppressors [8]. Many miRNAs, for example, miR-17, miR-21, and miR-373, are up-regulated in cancers and may function as oncogenes [9-11]. In HCCs, miR-122, miR-199a-5p, and miR-221 are regarded as tumor suppressors [12-14]. In various cancers, miR-491 acts as a tumor suppressor. For example, miR-491, mediated by Foxi1, functions as a tumor suppressor in the development of gastric cancer [15], and, in nasopharyngeal carcinoma, it is involved in cell cycle regulation and suppression of cell growth and invasion [16]. In non-small cell lung cancer, miR-491 suppresses cell proliferation and invasion by inhibiting IGF2BP1 [17]. Moreover, miR-491 levels are low in human liver cancers, in which it may function as a tumor suppressor [18]. However, the mechanism by which miR-491 functions in liver cancers is incompletely understood.

Epidermal growth factor receptor (EGFR), a tyrosine kinase, is involved in diverse cellular functions, including proliferation, angiogenesis, and suppression of cell death [19]. Signal transduction and activator of transcription 3 (STAT3), a transcription factor required for cellular transformation, has pro-tumorigenic functions, including promotion of tumor cell proliferation, survival, invasion, metastasis, and angiogenesis, is considered to be an oncogene [20]. Increasing the levels of EGFR results in activation of STATs, which promote cell survival and contribute to tumor growth [21-23]. However, how the EGFR regulation of STAT3 influences cancer stem cell (CSC)-like properties and metastasis of HCC cells is unclear.

In the present study, we sought to determine if miR-491 functions as a tumor suppressor gene in HCCs. We found that the levels of miR-491 were down-regulated in HCC specimens relative to specimens of adjacent normal liver. Prediction tools for miRNA–mRNA identified EGFR as a target of miR-491 and indicated that miR-491 directly regulates EGFR. The knockdown of miR-491 in HepG2 cells increased the levels of p-STAT3 and EGFR. Reduced expression of miR-491 increased the levels of CSC-like markers (Bmi-1, Oct-4, CD133, and EPCAM) and the levels of metastasis markers (MMP-9 and MMP-2) and enhanced the acquisition of CSC-like properties, neoplastic capacity, and migration; these effects were blocked by STAT3 siRNA. In contrast, over-expression of miR-491 decreased the levels of Bmi-1, Oct-4, CD133, EPCAM, MMP-9, and MMP-2 and inhibited the acquisition of CSC-like properties, neoplastic capacity, and migration of MHCC97H cells; these effects were blocked by up-regulation of STAT3 levels. Thus, miR-491 blocking STAT3 activation via EGFR is involved in metastasis of hepatocellular carcinoma cells through inhibiting CSC-like properties. In sum, miR-491 functions as a tumor suppressor in HCCs and provides a mechanism for preventing metastasis of HCCs.

RESULTS

In HCC specimens, miR-491 levels are down-regulated, and levels of EGFR and p-STAT3 are up-regulated

To assess the functions of miR-491, EGFR, and STAT3 activation in HCCs, we determined the levels of miR491, EGFR, and phospho-STAT3 in 15 HCC tissues and paired adjacent normal tissues by qRT-PCR and Western blots. The results showed that, in HCC specimens, the levels of miR-491 were down-regulated, and the levels of EGFR and p-STAT3 were up-regulated, relative to values of paired adjacent normal tissues (Figure 1A, 1B, and 1C). There was a negative correlation between miR-491 and EGFR and phospho-STAT3 (Figure 1D). The levels of miR-491 in three human HCC cell lines with different metastatic potential were measured; miR-491 expression was decreased in relation to increasing metastatic potential. miR-491 levels in the low-malignant liver HepG2 cells were higher than those in MHCC97L (moderately malignant) and MHCC97H (highly malignant) cells (Figure 1E). The clinicopathological characteristics of the patients are listed in Table 1. The levels of miR-491 were lower in tumors of higher clinical stages but were not associated with age (0.713), gender (0.545), or other factors. Thus, in HCC specimens, miR-491 levels are down-regulated, EGFR levels are up-regulated, and STAT3 is activated, changes that correlate with the clinical stage of HCCs.

miR-491 is involved in increases of EGFR levels and the activation of STAT3 in HCC cells

To confirm that miR-491 is associated with the expression of EGFR and the activation of STAT3, HepG2 cells were transfected with anti-miR-491 or anti-miR-NC for 24 h. Anti-miR-491 decreased miR-491 levels (Figure 2A). Knockdown of miR-491 elevated the levels of EGFR and phospho-STAT3, but there was no appreciable change in total STAT3 levels (Figure 2B and 2C). In MHCC97H cells transfected with miR-491-mimic for 24 h, the levels of miR-491 were increased by transfection with miR-491 mimic (Figure 2D). Up-regulation of miR-491 levels suppressed the levels of EGFR and phospho-STAT3 (Figure 2E and 2F). Thus, in HCC cells, miR-491 inhibits EGFR and phospho-STAT3 expression.

In HCC cells, miR-491 directly targets the EGFR 3'-UTR

miR-491 inhibits expression of EGFR [24]. To determine if miR-491 targets EGFR mRNA in HCC cells, the potential binding site of miR-491 for the 3′-UTR of EGFR (Figure 3A) was predicted via microRNA.org (http://www.microrna.org), TargetScan (www.targetscan.org), and miRDB (www.mirdb.org), and luciferase reporter assays were conducted. In HepG2 cells co-transfected with the pGL3-EGFR 3′UTR wild type or mutant Luc construct and anti-miR-491, down-regulation of miR-491 enhanced the luciferase activities of the EGFR 3′UTR-wt Luc construct (Figure 3B). In addition, the luciferase activities of the wild type construct were lower than those for control MHCC97H cells co-transfected with an miR-491 mimic (Figure 3C). These results indicate that miR-491 directly targets the EGFR 3'-UTR in HCC cells.

EGFR blocks the effect of miR-491 on the activation of STAT3 in HCC cells

To establish that EGFR is associated with miR-491 in the activation of STAT3, HepG2 cells were transfected with anti-miR-491without or with co-transfection with EGFR siRNA for 24 h. Down-regulation of miR-491 elevated the levels of EGFR and phospho-STAT3; the effects were reversed by co-transfecting cells with EGFR siRNA (Figure 4A and 4B). In contrast, after MHCC97H cells were transfected with miR-491-mimic without or with co-transfection with pEGFP-EGFR for 24 h, the

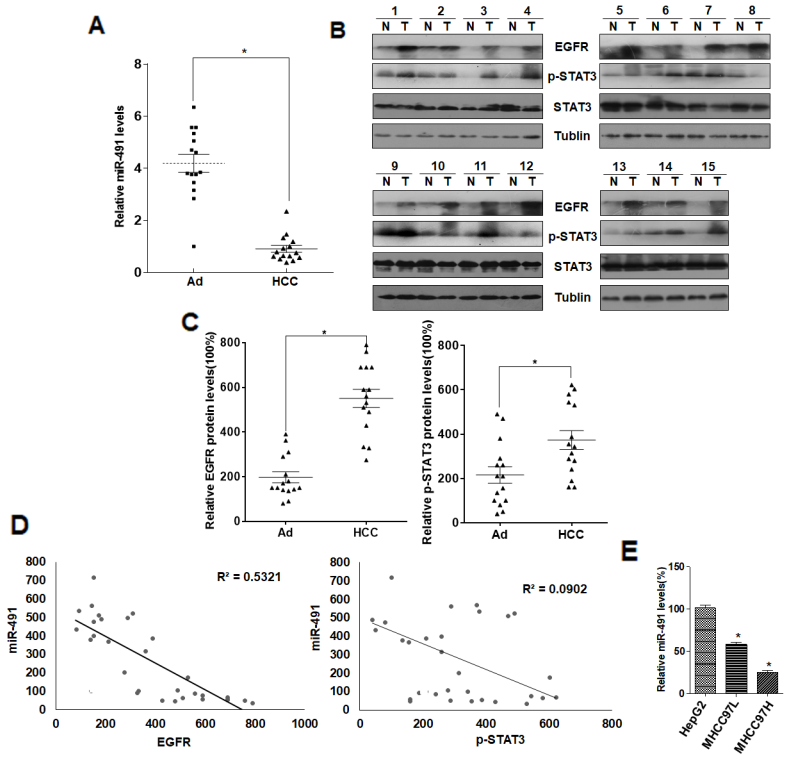

Figure 1: miR-491 levels are down-regulated and the levels of EGFR and p-STAT3 are up-regulated in HCC specimens. 15 HCC tissues and paired adjacent normal tissues were collected. **(A)** The levels of miR-491 were determined by qRT-PCR (means ± SD, n = 3). $^{*}P < 0.05$ different from adjacent normal tissues. **(B)** Western blots were performed, and **(C)** the relative protein levels (means ± SD, n = 3) of EGFR and p-STAT3 were determined. $^{*}P < 0.05$ different from adjacent normal tissues. **(D)** The relationship of miR-491 levels to EGFR ($R^2 = 0.5321$) and to p-STAT3 ($R^2 = 0.0902$) in HCC tissues and adjacent normal tissues. **(E)** The levels of miR-491 were determined by qRT-PCR for HCC cell lines with different aggressive characteristics (means ± SD, n = 3), $^{*}P<0.05$, different from HepG2 cells.

Table 1: Correlation between the levels of miR-491 and the clinicopathological characteristics of HCC.

Characteristic	miR-491		P
	Low (N=9)	High (N=6)	
Age (years)			
≦50	6	4	0.713
>50	3	2	
Gender			
Male	5	4	0.545
Female	4	2	
HBsAg[a]			
Positive	5	3	0.622
Negative	4	3	
Serum AFP[b] (ng/ml)			
<200	3	4	0.287
>200	6	2	
Cirrhosis			
Yes	5	2	0.378
No	4	4	
Tumor size			
<3 cm	2	4	0.119
≥3 cm	7	2	
Multinodular tumor			
Yes	5	2	0.378
No	4	4	
TNM stage			
I-II	2	5	0.035*
III-IV	7	1	

[a] HBsAg: surface antigen of the hepatitis B virus.
[b] AFP: α-fetoprotein, a marker for liver cancer. *$P<0.05$

increases of miR-491 levels suppressed the levels of EGFR and phospho-STAT3 (Figure 4C and 4D). However, the effects of miR-491 on inhibiting EGFR and phospho-STAT3 expression were reversed by up-regulation of EGFR; cells co-transfected with the miR-491-mimic and the empty vector did not show this effect (Figure 4C and 4D). Hence, in HCC cells, miR-491 regulates STAT3 activation via EGFR.

STAT3 is involved in the effect of miR-491 on the acquisition of CSC-like properties in HCC cells

The functions of miR-491 in the acquisition of CSC-like properties were investigated. Spheroids were formed to confirm the capacity of self-renewal and initiation of tumors, which are characteristics of stem cells. The key 'stemness' genes, *Oct-4, Bmi1, CD133,* and *EPCAM* are expressed in CSCs from various cancers [25]. After HepG2 cells were transfected with anti-miR-491, the levels of Oct-4, Bmi1, CD133 and EPCAM were elevated, and the formation of spheroids was enhanced; these effects were reversed by co-transfection of cells with STAT3 siRNA (Figure 5A-5E). In addition, the increased levels of p-STAT3 induced by inhibiting miR-491 were reduced by STAT3 siRNA (Supplementary Figure 1A and 1B). In contrast, for MHCC97H cells transfected with the miR-491-mimic or co-transfected with pEGFP-STAT3, the results showed that over-expression of miR-491 reduced

the expressions of Oct-4, Bmi1, CD133, and EPCAM and inhibited the formation of spheroids. These effects were reversed by over-expression of STAT3 (Figure 5F-5J). Also, the expressions of p-STAT3 and STAT3 were increased by pEGFP-STAT3 (Supplementary Figure 1C and 1D). Thus, in HCC cells, miR-491 blocked the acquisition of CSC-like properties via STAT3.

miR-491, acting via STAT3, influences the neoplastic, migration, and invasion capacities of HCC cells

Based on the data showing that miR-491-mediated STAT3 is involved in the acquisition of CSC-like properties of HCC cells, we determined if the regulation of STAT3 by miR-491 affected the neoplastic capacity,

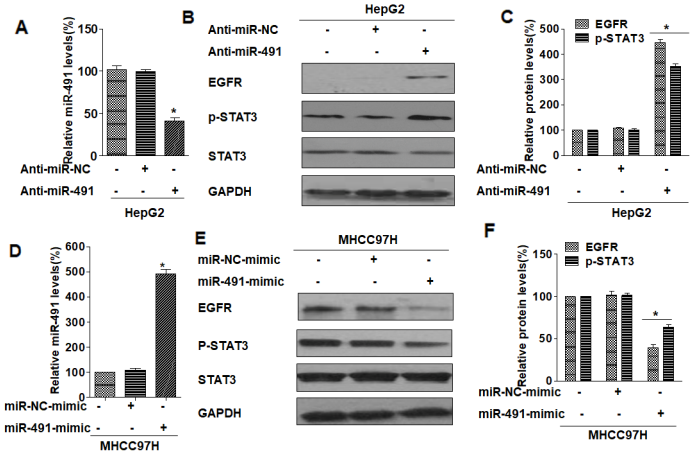

Figure 2: miR-491 is involved in the regulation of EGFR levels and the activation of STAT3 in HCC cells. Densities of bands were quantified by Eagle Eye II software. GAPDH levels, measured in parallel, served as controls. HepG2 cells were transfected with 150 nM anti-miR-NC or anti-miR-491 for 24 h. **(A)** Levels of miR-491 were determined by qRT-PCR (means ± SD, n = 3). **(B)** Western blots were performed, and **(C)** the relative levels of VEGF and p-STAT3 were determined (means ± SD, n = 3), $^{*}P<0.05$ difference from HepG2 cells in the absence of anti-miR-491. MHCC97H cells were transfected with 150 nM miR-NC-mimic or miR-491-mimic for 24 h. **(D)** Levels of miR-491were determined by qRT-PCR (means ± SD, n= 3). **(E)** Western blots were performed, and **(F)** the relative levels of VEGF and p-STAT3 were determined (means ± SD, n = 3), $^{*}P<0.05$ difference from MHCC97H cells in the absence of the miR-491-mimic.

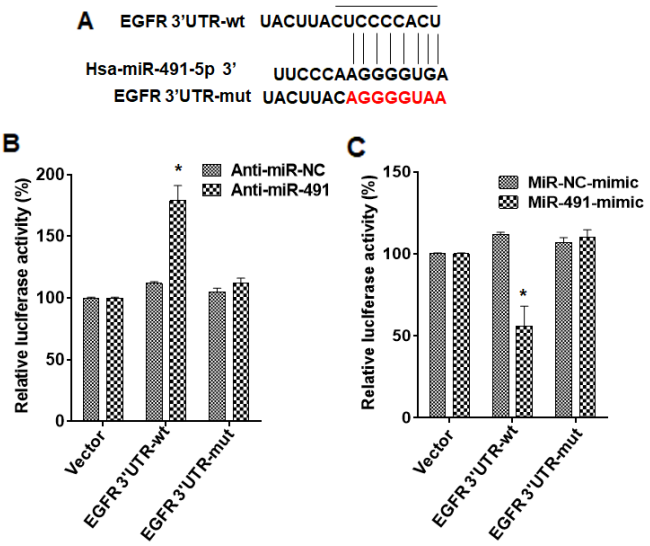

Figure 3: miR-491 regulates the transcriptional levels of EGFR in HCC cells. (A) The binding sites of miR-491 in the EGFR 3′UTR were predicted via bioinformatics tools. HepG2 cells were co-transfected with the pGL3-EGFR 3′UTR-Luc wild or mutant construct and 150 nM anti-miR-491 for 24 h. **(B)** Luciferase activity was measured and normalized to Renilla luciferase activity (means ± SD, n = 3), $^{*}P<0.05$ difference from HepG2 cells in the absence of anti-miR-491. MHCC97H cells were co-transfected with the pGL3-EGFR 3′UTR-Luc wild or mutant construct and with 150 nM miR-491-mimic for 24 h. **(C)** Luciferase activity was measured and normalized according to Renilla luciferase activity (means ± SD, n = 3), $^{*}P<0.05$ difference from MHCC97H cells in the absence of miR-491-mimic.

migration, and invasion of HCC cells. After HepG2 cells were transfected with anti-miR-491, the levels of MMP-9 and MMP-2 were elevated, and the capacities for colony formation, migration, and invasion were enhanced, but these effects were reversed by co-transfecting with STAT3 siRNA (Figure 6A-6F). In contrast, for MHCC97H cells, over-expression of miR-491 reduced the expressions of MMP-9 and MMP-2 and inhibited the capacities for colony formation, migration, and invasion; these effects were reversed by the elevated STAT3 levels in MHCC97H cells co-transfected with pEGFP-STAT3 (Figure 6G-6L). Thus, miR-491 inhibits the neoplastic, migration, and invasion capacities of HCC cells via STAT3.

DISCUSSION

HCC is a common malignancy worldwide,with over 782,000 newly diagnosed cases per year. As the second most frequent cause of cancer deaths, HCC is responsible for 746,000 cancer deaths annually, half of which occur in China [26, 27]. Although hepatitis B virus infection is the most relevant risk factor for HCC in China, a lack of sensitive and specific biomarkers for the early detection of this disease has impeded the development and effectiveness of therapeutic strategies. Therefore, there is a need to identify biomarkers for discovery of HCC before it becomes clinically detectable and has progressed to lethal, advanced stages. To our knowledge, the present report is the first to address the relationship between miR-491 and CSCs in HCC and to investigate the underlying molecular mechanisms.

miRNAs are evolutionarily conserved, small-noncoding RNAs involved in the regulation of gene expression and protein translation [7]. Altered expression of circulating miRNAs is associated with various diseases, including HCC [28, 29]. As determined in our previous study, miR-491, an anticancer miRNA [18], is associated with metastasis and the epithelial-mesenchymal transition (EMT) of HCC [30]. In the present research, we found that the levels of miR-491 in HCC tissues were lower than those in corresponding normal tissues. In addition, of three HCC cell lines (HepG2, MHCC97L, and MHCC97H), the weakly malignant HepG2 cells expressed the highest level of miR-491, whereas the highly malignant MHCC97H cells expressed the lowest level. These results indicate that miR-491 is a tumor suppressor. To determine the relationship between miR-491 and malignant potential, we used HepG2 and MHCC97H cell lines for knockdown and overexpression of miR-491, respectively.

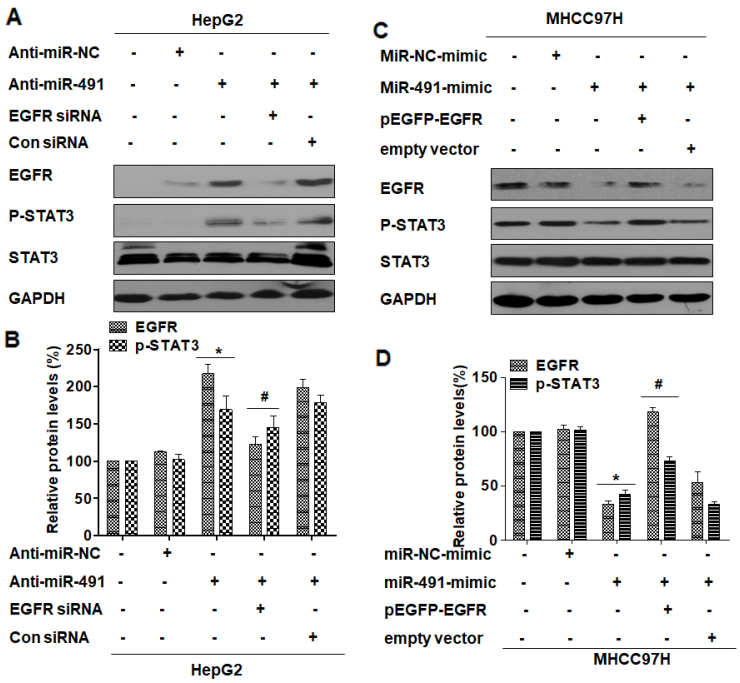

Figure 4: EGFR blocks the effect of miR-491 on the activation of STAT3 in HCC cells. Densities of bands were quantified by Eagle Eye II software. GAPDH levels, measured in parallel, served as controls. HepG2 cells were transfected with 150 nM anti-miR-NC or with anti-miR-491 without or with co-transfection with 30 nM EGFR-siRNA or con siRNA for 24 h. **(A)** Western blots were performed, and **(B)** relative protein levels of EGFR and p-STAT3 were determined (means ± SD, n = 3), $^{*}P<0.05$ difference from HepG2 cells in the absence of anti-miR-491, $^{\#}P<0.05$ difference from HepG2 cells treated with anti-miR-491 in the absence of EGFR-siRNA. MHCC97H cells were transfected with 150 nM miR-491-mimic without or with co-transfection with 10 μg pEGFP-EGFR or empty vector for 24 h. **(C)** Western blots were performed, and **(D)** relative protein levels of EGFR and p-STAT3 were determined (means ± SD, n = 3), $^{*}P<0.05$ difference from MHCC97H cells in the absence of miR-491-mimic, $^{\#}P<0.05$ difference from MHCC97H cells treated with miR-491-mimic in the absence of pEGFP-EGFR.

miRNAs have the capacity to inhibit translation and to induce mRNA degradation, predominantly through targeting of the 3′-UTRs of mRNAs [31]. In ovarian carcinomas, miR-491-5p binds to the EGFR 3′-UTR to mediate a repressive effect on protein expression [24]. miR-491 is predicted to down-regulate oncogenic targets, such as TGFβ, BCLXW, BCL-Xl, and STATs, and to have a negative effect on the STAT3 and PI3K/Akt signaling

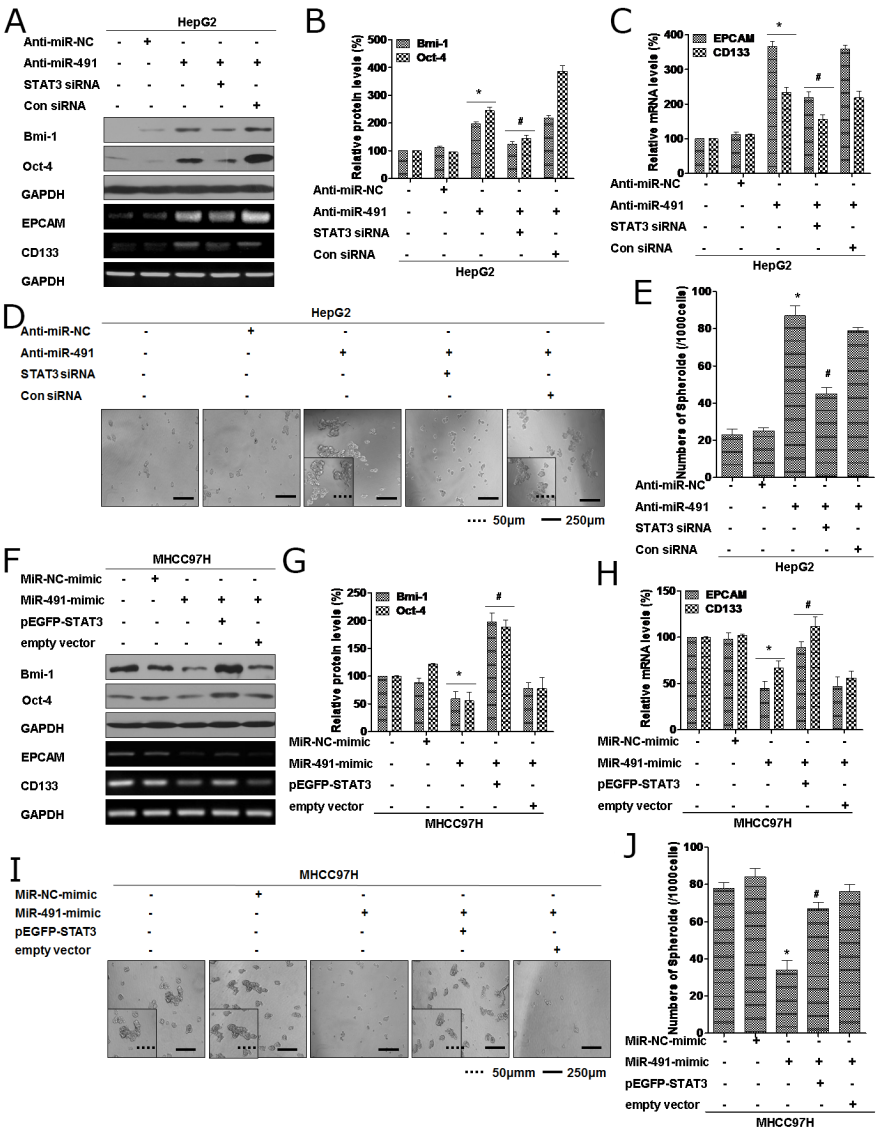

Figure 5: STAT3 is involved in the effect of miR-491 on the acquisition of CSC-like properties in HCC cells. Densities of bands were quantified by Eagle Eye II software. GAPDH levels, measured in parallel, served as controls. HepG2 cells were transfected with 150 nM anti-miR-NC or with anti-miR-491, without or with co-transfection with STAT3-siRNA or con siRNA (30 nM) for 24 h. **(A)** Western blot (upper) and RT-PCR (below) analyses were performed, and **(B)** relative protein levels (means ± SD, n=3) of Bmi-1 and Oct-4 were determined, and **(C)** the mRNA levels of CD133 and EPCAM were determined by quantitative RT-PCR (means ± SD, n=3), $^{*}P<0.05$ difference from HepG2 cells in the absence of anti-miR-491, $^{\#}P<0.05$ difference from HepG2 cells treated with anti-miR-491 in the absence of STAT3-siRNA. **(D)** Free-floating, viable spheres formed from different treated cells and **(E)** their numbers (means ± SD, n=3) were quantified, bars=50 or 250 μM. $^{*}P<0.05$ difference from HepG2 cells in the absence of anti-miR-491, $^{\#}P<0.05$ difference from HepG2 cells treated with anti-miR-491 in the absence of STAT3-siRNA. MHCC97H cells were transfected with 150 nM miR-491-mimic or miR-NC-mimic or co-transfected with 10 μg pEGFP-STAT3 or empty vector for 24 h. **(F)** Western blot (upper) and RT-PCR (below) analyses were performed; **(G)** relative protein levels (means ± SD, n=3) of Bmi-1 and Oct-4 were determined; and **(H)** the mRNA levels of CD133 and EPCAM were determined by quantitative RT-PCR (means ± SD, n=3), $^{*}P<0.05$ difference from MHCC97H cells in the absence of miR-491-mimic, $^{\#}P<0.05$ difference from MHCC97H cells treated with miR-491-mimic in the absence of pEGFP-STAT3. **(I)** Free-floating, viable spheres formed from different treated cells and **(J)** their numbers (means ± SD, n=3) were quantified, bars=50 or 250 μM. $^{*}P<0.05$ difference from MHCC97H cells in the absence of miR-491-mimic, $^{\#}P<0.05$ difference from MHCC97H cells treated with miR-491-mimic in the absence of pEGFP-STAT3.

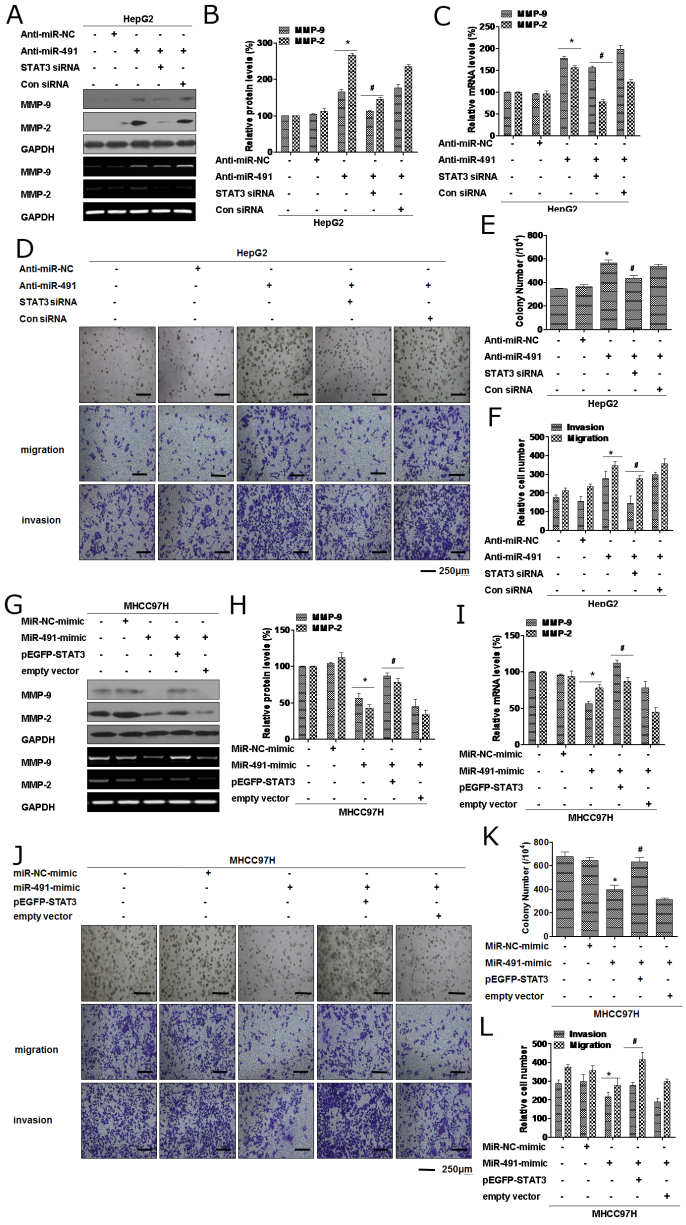

Figure 6: miR-491, acting via STAT3, influences the neoplastic capacity, migration, and invasion of HCC cells. Densities of bands were quantified by Eagle Eye II software. GAPDH levels, measured in parallel, served as controls. HepG2 cells were transfected with 150 nM anti-miR-NC or with anti-miR-491 without or with co-transfection with 30 nM STAT3-siRNA or con siRNA for 24 h. **(A)** Western blot (upper) and RT-PCR (below) analyses were performed; **(B)** relative protein levels (means ± SD, n=3) of MMP-9 and MMP-2 were determined; and **(C)** the mRNA levels of MMP-9 and MMP-2 were determined by quantitative RT-PCR (means ± SD, n=3), $^{*}P<0.05$ difference from HepG2 cells in the absence of anti-miR-491, $^{\#}P<0.05$ difference from HepG2 cells treated with anti-miR-491 in the absence of STAT3-siRNA. **(D)** Colony formation and was assessed in soft agar (upper); representative images of cell migration and invasion was assessed with Transwells; and **(E** and **F)** relative numbers of colony and migrating and invading cells (means ± SD, n = 3) were quantified, Bars= 250 μM. $^{*}P<0.05$ difference from HepG2 cells in the absence of anti-miR-491, $^{\#}P<0.05$ difference from HepG2 cells treated with anti-miR-491 in the absence of STAT3-siRNA. MHCC97H cells were transfected with 150 nM miR-491-mimic or miR-NC-mimic or co-transfected with 10 μg pEGFP-STAT3 or empty vector for 24 h. **(G)** Western blot (upper) and RT-PCR (below) analyses were performed; **(H)** relative protein levels (means ± SD, n=3) of MMP-9 and MMP-2 were determined; and **(I)** the mRNA levels of MMP-9 and MMP-2 were determined by quantitative RT-PCR (means ± SD, n=3), $^{*}P<0.05$ difference from MHCC97H cells in the absence of miR-491-mimic, $^{\#}P<0.05$ difference from MHCC97H cells treated with miR-491-mimic in the absence of pEGFP-STAT3. **(J)** Colony formation and was assessed in soft agar (upper); representative images of cell migration and invasion was assessed with Transwells; and **(K** and **L)** relative numbers of colonies and migrating and invading cells (means ± SD, n = 3) were quantified, Bars= 250 μM. $^{*}P<0.05$ difference from MHCC97H cells in the absence of miR-491-mimic, $^{\#}P<0.05$ difference from MHCC97H cells treated with miR-491-mimic in the absence of pEGFP-STAT3.

pathways [32]. In addition to miRNAs, another kind of ncRNAs, long non-coding RNAs (lncRNAs), are involved in cancer development. In colorectal cancer, lncRNA H19 functions as a sponge to promote the epithelial to mesenchymal transition [33], and it is implicated in gastric carcinogenesis [34]. In the present research, we found that, in HCC cells, miR-491 knockdown elevated the levels of EGFR and p-STAT3 and that miR-491 inhibited the luciferase activities of the pGL3-EGFR 3'UTR Luc construct. Thus, in HCC cells, miR-491 directly regulates EGFR.

EGFR is a multifunctional membrane glycoprotein found in a variety of tissue types. Overexpression of EGFR leads to excessive cell growth and malignancy [35]. STATs are transcription factors activated by peptide ligands such as cytokines and growth factors, including EGF [36]. In the present study, we found that miR-491 blocks p-STAT3 expression and that miR-491 targets EGFR. Thus, we hypothesized that miR-491 regulates STAT3 through EGFR. Over-expression of miR-491 inhibited the levels of EGFR and p-STAT3, but the p-STAT3 levels were reversed by ectopic expression of EGFR in HCCs. Thus, in HCC cells, miR-491 regulates STAT3 activation via EGFR.

In a variety of human cancers, miR-491 functions as a tumor suppressor. In colorectal cancer cells, it induces apoptosis by targeting Bcl-XL [37]. In pancreatic cancer cells, it targets both TP53- and Bcl-XL-induced apoptosis through the mitochondria-mediated pathway [32]. In addition, miR-491 functions as an anti-metastasis gene by targeting MMP9 and G-protein-coupled receptor kinase-interacting protein 1 [30, 38]. It also attenuates malignant properties by targeting oncogenes, such as *EGFR*, *Wnt*, and *GIT-1* [38, 39]. In cancer cells, these genes elevate CSC-like properties [40]. Nevertheless, the molecular mechanisms underlying in the repressive effects on CSC-like properties induced by miR-491 are complicated. STAT3 activity is required for maintenance of the stem-like characteristics of glioblastoma stem cells (GSCs) [41]. Moreover, IL-6 and EZH2 activate STAT3 signaling to maintain the self-renewal and tumorigenic potential of GSCs [42, 43]. STAT3 activation is essential for maintenance of TNBC stem cells [44]. Its activation also orients carcinoma cells towards a CSC phenotype [45], confirming the involvement of STAT3 signaling in acquisition of stem cell-like characteristics. In the present study, we found that, in HepG2 cells, knockdown of miR-491 enhanced the acquisition of CSC-like properties

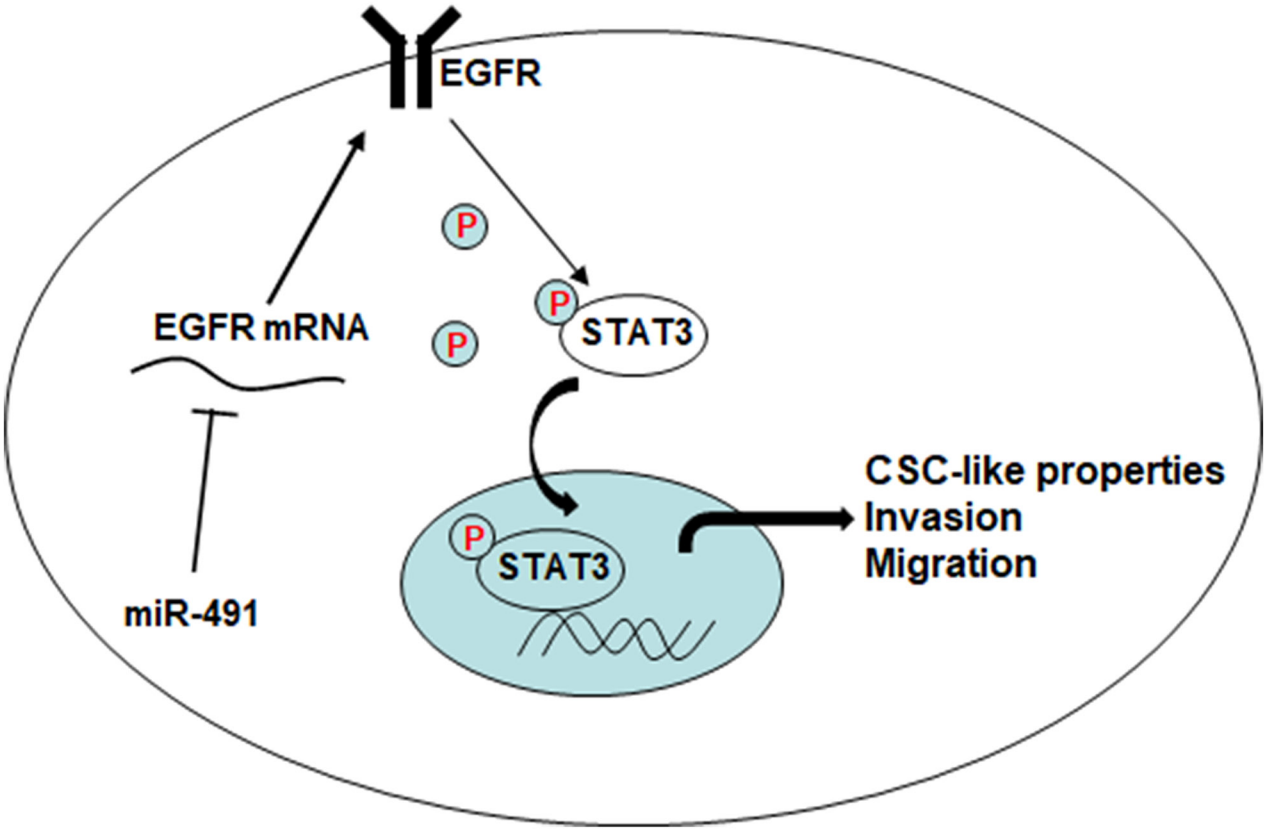

Figure 7: miR-491 via EGFR/STAT3 suppresses the metastasis of HCC cells. In HCC cells, miR-491 influences CSC-like properties and metastasis by blocking the activation of STAT3 via EGFR.

and that inhibition of STAT3 reversed this process. On the contrary, over-expression of miR-491 blocked the acquisition of CSC-like properties, and ectopic expression of STAT3 reversed these effects. These results indicate that, in HCC cells, miR-491 influences the acquisition of CSC-like properties through inhibiting STAT3.

The EMT and CSC characteristics endow epithelial cells with enhanced neoplastic properties, and EMT phenotypes are associated with the invasion and migration of cancer cells [46]. In cancer cells, the EMT and CSCs are implicated in tumor invasion and metastasis [47]. Levels of miR-491-5p are lower in highly invasive oral squamous cell carcinoma lines relative to their corresponding, less-invasive parental cells. Further, miR-491-5p suppresses migration, invasion, and metastasis of oral cancer cells, mainly via targeting GIT1 to affect FAK and ERK1/2 signaling [38]. In glioblastoma multiforme cells, miR-491-5p inhibits expression of MMP9 and the capacity for invasion [48]. As established in the present study, the effects of miR-491 on neoplastic capacity of HCC cells were mediated through regulating CSCs. Moreover, miR-491 inhibited neoplastic and metastatic capacity in HCC cells via STAT3. Thus, miR-491 is involved in the neoplastic and metastatic capacity of HCC cells through STAT3.

In summary, in HCC specimens, miR-491 levels were down-regulated, EGFR levels were up-regulated, and STAT3 was activated, indicating that, for HCC patients, miR-491, as a tumor suppressor, may be a prognostic indicator. Further, miR-491 regulates EGFR. Moreover, the effects of miR-491 on inhibiting phospho-STAT3 expression are reversed by the up-regulation of EGFR, which indicates that miR-491 regulates STAT3 activation via EGFR. Further, in HCC cells, STAT3 blocks the effects of miR-491 on the acquisition of CSC-like properties, neoplastic capacity, and migration. By blocking the activation of STAT3 via EGFR, miR-491 influences CSC-like properties and metastasis of HCC cells (Figure 7). Our results concerning miR-491 functionality and molecular mechanisms provide a new perspective for miRNA-directed diagnostics and drug targets for HCC.

MATERIALS AND METHODS

Cell culture and reagents

HepG2 cells (an HCC cell line with very low migratory capacity) [49], MHCC97H cells, and MHCC97L cells (HCC cell lines with high and low migratory potential, respectively) [50], were purchased from the Shanghai Institute of Cell Biology, Chinese Academy of Sciences (Shanghai, China). These cells were maintained in Dulbecco's modified eagle medium (DMEM) with 10% fetal bovine serum (FBS, Life Technologies/Gibco, Grand Island, NY, USA), 100 U/mL penicillin, and 100 μg/mL streptomycin (Life Technologies/Gibco, Gaithersburg, MD) and incubated in 5% CO_2 at 37 °C. Tyrphostin AG490 was purchased from Beyotime Institute of Biotechnology (Shanghai, China). All other reagents used were of analytical grade or the highest grade available.

Patients and tissue samples

This study was reviewed and approved by Medical Ethics Committee of the Second Affiliated Hospital of Nanjing Medical University. A total of 15 Chinese HCC patients had effective liver resections for primary tumors between May 2009 and March 2012 at The Second Affiliated Hospital of Nanjing Medical University. The approbation of our ethics committees and the participants' written informed consent are listed in the section of ethics committees. The criteria for the patient cohort were (i) having a distinctive pathological diagnosis of HCC; (ii) surgical resection, defined as complete resection of all tumor nodules with the cut margin being free of cancer by histological examination; and (iii) having complete clinicopathological data. An exclusion criterion was prior anticancer treatment before liver resection. No patients had extrahepatic metastases when they experienced hepatectomies. The patients' clinicopathological characteristics are listed in Table 1.

Western blots

Western blot analyses to assess protein expression were accomplished as described previously [51]. Anti-glyceraldehyde 3-phosphate dehydrogenase (GAPDH) was purchased from Sigma, the antibodies for phospho-STAT3 and STAT3 were purchased from Cell Signaling Technology (Beverly, MA), and EGFR, Bmi-1, Oct-4, MMP-9, and MMP-2 were from Abcam, (Cambridge, MA). For densitometric analyses, the bands on the blots were measured by Eagle Eye II.

Reverse-transcriptase polymerase chain reaction (RT-PCR)

Total cellular and tissue RNA was isolated by use of TRIzol (Invitrogen) according to the manufacturer's recommendations. Total RNA (2 μg) was transcribed into cDNA by the use of AMV reverse transcriptase (Promega, Madison, Wisconsin, USA). All primers used are listed in Supplementary Table 1. PCR was evaluated by checking the products on 2% w/v agarose gels. GAPDH acts as the control. For densitometric analyses, the mRNA bands on the gels were measured by Eagle Eye II.

Real-time RT-PCR analysis (qRT-PCR)

Total cellular RNA was isolated by use of Trizol (Invitrogen, Carlsbad, CA, USA) according to the manufacturer's recommendations. Briefly, total RNA was prepared, and its concentration and integrity were assessed

as previously described [52]. For detection of mature miR-491, 2 μg of total RNA, miR-491-specific stem-loop RT primers, and MMLV reverse transcriptase (Promega) were used in reverse transcription following the manufacturer's protocol. The sequences of mature miR-491 were from Sanger miRBase (http://microrna.sanger.ac.uk/sequences/). The gene-specific primers were as follows: miR-491-F, 5′-ACACTCCAGCTGGGAGTGGGGAACCCTTCC -3′; miR-491-R, 5′-TGGTGTCGTGGAGTCG-3′; U6-F, 5′-*CGCTTCGGCAGCACATATACTAAAATTGGAAC*-3′, and U6-R, 5′-*GCTTCACGAATTTGCGTGTCATCCTTGC*-3′. Quantitative real-time PCR was performed with an Applied Biosystems 7300HT machine and Maxima™ SYBR Green/ROX qPCR Master Mix (Fermentas). U6 snRNA was used as a control. The relative gene expression was calculated by the formula $2^{-(\Delta\Delta Ct)}$[52].

Cell transfection

STAT3 and EGFR siRNA were purchased from Santa Cruz Biotechnology. miR-491 inhibitor, miR-491 mimic, and miRNA negative control were synthesized by RiBoBio (Guangzhou, China). The STAT3 or EGFR sequence was subcloned into a pEGFP vector (Genechem, Shanghai, China). 5×10^5 cells were grown on 6-well plates and transfected by using Lipofectamine 2000 (Invitrogen), according to the manufacturer's instructions. The preparations were incubated at room temperature for 30 min. At 24 h after transfection, cells were treated and subsequently harvested for qRT-PCR or Western blot analyses.

Transwell assays

The invasive and migratory capacities of HCC cells were evaluated by use of Transwell chambers with 8-μm pore filters (Corning, Inc., Corning, NY, USA). The chambers were coated with Matrigel (BD Biosciences, Franklin Lakes, NJ, USA) for determination of invasive ability. For the migration test, no Matrigel was added. After 24 h of transfection, 5×10^4/100 μL cells were plated on the upper chambers coated with or without 35 μL of Matrigel in serum-free medium. DMEM medium containing 10% FBS was added to the lower chambers as a chemoattractant. After incubation for 24 h at 37 °C, non-migrating or non-invading cells were removed with cotton swabs. Cells that migrated or invaded to the bottom of the membrane were fixed with 4% paraformaldehyde, stained with crystal violet solution for 30 min, and visualized under a microscope (high-power field). The numbers of cells counted in five random fields were averaged.

Luciferase reporter assay

The pGL3-EGFR 3'UTR (wide type, wt)-Luc construct was purchased from GeneChem (Shanghai, China). The plasmid phRL-tk (used as internal control for transfection efficiency and cytotoxicity of test chemicals) containing the Renilla luciferase gene was purchased from Promega (Madison, WI, USA). An miR-491 mimic or miR-491 inhibitor was co-transfected with the reporter constructs into cells by Lipofectamine 2000 reagent (Invitrogen)-mediated gene transfer according to the manufacturer's protocol. Approximately 12 h after transfection, the cells were washed three times with PBS (pH 7.4). Then the cells were lysed with 1× passive lysis buffer (Promega). The lysates from each well were analyzed in a 96-well plate illuminometer (Berthold Detection System, Pforzheim, Germany). The amounts of luciferase and Renilla luciferase were measured with the Dual-Luciferase Reporter Assay System Kit (Promega) following the manufacturer's instructions. Transfection experiments were performed in quadruplicate and were repeated at least three times. The relative luciferase activity was normalized to Renilla luciferase activity, as reported previously [51].

Anchorage-independent growth

Soft-agar dishes were prepared with under-layers of 0.70% agarose in DMEM medium supplemented with 10% FBS. To test their capacity for colony growth in soft agar, cells were plated in triplicate at a density of 1×10^4 in 2 ml of 0.35% agarose over the agar base. The cultures were fed every three days; after 14 days, the colonies containing > 30 cells, that is, those with a diameter of >30 μm, were counted.

Spheroid formation

The cells (1×10^4) were suspended in non-adherent dishes (Costar). To serum-free medium containing DMEM/F-12 (Life Technologies/Gibco), 10 ng/ml of human recombinant basic fibroblast growth factor (R&D Systems, Shanghai, China), and 10 ng/ml of epidermal growth factor (R&D Systems) were added. Cells were grown for 10 days and fed every 48 h. The total spheres were counted under a microscope (Olympus, Tokyo, Japan).

Statistical analyses

All experiments were performed at least three times in triplicate for each group. The results are presented as means ± SD. Comparisons of means among multiple groups were performed by one-way analysis of variance (ANOVA), and a multiple-range least significant difference (LSD) was used for inter-group comparisons. Statistical significance was reached if $P < 0.05$. All statistical analyses were performed with SPSS 16.0.

Ethics approval and consent to participate

The study protocol was approved by the Medical Ethics Commission of Nanjing Medical University. The approbation of the ethics committees and the participants'

written informed consent was listed in the section of ethics committees.

ACKNOWLEDGMENTS

The authors thank Donald L. Hill (University of Alabama at Birmingham, USA), an experienced, English-speaking scientific writer for editing.

CONFLICTS OF INTEREST

The authors declare no conflict of interest.

FUNDING

This work was supported by the Natural Science Foundations of China (81273114 and 81272713) and by a project funded by the Priority Academic Program Development of Jiangsu Higher Education Institutions (2014).

REFERENCES

1. Zhang T, Huang Y, Liu W, Meng W, Zhao H, Yang Q, Gu SJ, Xiao CC, Jia CC, Zhang B, Zou Y, Li HP, Fu BS. Overexpression of zinc finger protein 687 enhances tumorigenic capability and promotes recurrence of hepatocellular carcinoma. Oncogenesis. 2017; 6: e363. https://doi.org/10.1038/oncsis.2017.63.
2. Zuo TT, Zheng RS, Zhang SW, Zeng HM, Chen WQ. Incidence and mortality of liver cancer in China in 2011. Chin J Cancer. 2015; 34: 508-13. https://doi.org/10.1186/s40880-015-0056-0.
3. Livraghi T, Makisalo H, Line PD. Treatment options in hepatocellular carcinoma today. Scand J Surg. 2011; 100: 22-9.
4. Dhanasekaran R, Limaye A, Cabrera R. Hepatocellular carcinoma: current trends in worldwide epidemiology, risk factors, diagnosis, and therapeutics. Hepat Med. 2012; 4: 19-37. https://doi.org/10.2147/HMER.S16316.
5. Calin GA, Croce CM. MicroRNA signatures in human cancers. Nat Rev Cancer. 2006; 6: 857-66. https://doi.org/10.1038/nrc1997.
6. Inui M, Martello G, Piccolo S. MicroRNA control of signal transduction. Nat Rev Mol Cell Biol. 2010; 11: 252-63. https://doi.org/10.1038/nrm2868.
7. Bartel DP. MicroRNAs: genomics, biogenesis, mechanism, and function. Cell. 2004; 116: 281-97.
8. Zhao X, Yang Z, Li G, Li D, Zhao Y, Wu Y, Robson SC, He L, Xu Y, Miao R, Zhao H. The role and clinical implications of microRNAs in hepatocellular carcinoma. Sci China Life Sci. 2012; 55: 906-19. https://doi.org/10.1007/s11427-012-4384-x.
9. Oksuz Z, Serin MS, Kaplan E, Dogen A, Tezcan S, Aslan G, Emekdas G, Sezgin O, Altintas E, Tiftik EN. Serum microRNAs; miR-30c-5p, miR-223-3p, miR-302c-3p and miR-17-5p could be used as novel non-invasive biomarkers for HCV-positive cirrhosis and hepatocellular carcinoma. Mol Biol Rep. 2015; 42: 713-20. https://doi.org/10.1007/s11033-014-3819-9.
10. Gu H, Guo X, Zou L, Zhu H, Zhang J. Upregulation of microRNA-372 associates with tumor progression and prognosis in hepatocellular carcinoma. Mol Cell Biochem. 2013; 375: 23-30. https://doi.org/10.1007/s11010-012-1521-6.
11. Wu W, He X, Kong J, Ye B. Mir-373 affects human lung cancer cells' growth and its E-cadherin expression. Oncol Res. 2012; 20: 163-70.
12. Nassirpour R, Mehta PP, Yin MJ. miR-122 regulates tumorigenesis in hepatocellular carcinoma by targeting AKT3. PLoS One. 2013; 8: e79655. https://doi.org/10.1371/journal.pone.0079655.
13. Callegari E, Elamin BK, D'Abundo L, Falzoni S, Donvito G, Moshiri F, Milazzo M, Altavilla G, Giacomelli L, Fornari F, Hemminki A, Di Virgilio F, Gramantieri L, et al. Anti-tumor activity of a miR-199-dependent oncolytic adenovirus. PLoS One. 2013; 8: e73964. https://doi.org/10.1371/journal.pone.0073964.
14. Yang X, Yang Y, Gan R, Zhao L, Li W, Zhou H, Wang X, Lu J, Meng QH. Down-regulation of mir-221 and mir-222 restrain prostate cancer cell proliferation and migration that is partly mediated by activation of SIRT1. PLoS One. 2014; 9: e98833. https://doi.org/10.1371/journal.pone.0098833.
15. Sun R, Liu Z, Tong D, Yang Y, Guo B, Wang X, Zhao L, Huang C. miR-491-5p, mediated by Foxi1, functions as a tumor suppressor by targeting Wnt3a/beta-catenin signaling in the development of gastric cancer. Cell Death Dis. 2017; 8: e2714. https://doi.org/10.1038/cddis.2017.134.
16. Zhang Q, Li Q, Xu T, Jiang H, Xu LG. miR-491-5p suppresses cell growth and invasion by targeting Notch3 in nasopharyngeal carcinoma. Oncol Rep. 2016; 35: 3541-7. https://doi.org/10.3892/or.2016.4713.
17. Gong F, Ren P, Zhang Y, Jiang J, Zhang H. MicroRNAs-491-5p suppresses cell proliferation and invasion by inhibiting IGF2BP1 in non-small cell lung cancer. Am J Transl Res. 2016; 8: 485-95.
18. Ishida H, Tatsumi T, Hosui A, Nawa T, Kodama T, Shimizu S, Hikita H, Hiramatsu N, Kanto T, Hayashi N, Takehara T. Alterations in microRNA expression profile in HCV-infected hepatoma cells: involvement of miR-491 in regulation of HCV replication via the PI3 kinase/Akt pathway. Biochem Biophys Res Commun. 2011; 412: 92-7. https://doi.org/10.1016/j.bbrc.2011.07.049.
19. Pal HC, Sharma S, Strickland LR, Agarwal J, Athar M, Elmets CA, Afaq F. Delphinidin reduces cell proliferation and induces apoptosis of non-small-cell lung cancer cells by targeting EGFR/VEGFR2 signaling pathways. PLoS

One. 2013; 8: e77270. https://doi.org/10.1371/journal.pone.0077270.

20. Rathinavelu A, Narasimhan M, Muthumani P. A novel regulation of VEGF expression by HIF-1alpha and STAT3 in HDM2 transfected prostate cancer cells. J Cell Mol Med. 2012; 16: 1750-7. https://doi.org/10.1111/j.1582-4934.2011.01472.x.

21. Lindemann C, Hackmann O, Delic S, Schmidt N, Reifenberger G, Riemenschneider MJ. SOCS3 promoter methylation is mutually exclusive to EGFR amplification in gliomas and promotes glioma cell invasion through STAT3 and FAK activation. Acta Neuropathol. 2011; 122: 241-51. https://doi.org/10.1007/s00401-011-0832-0.

22. Torres AF, Nogueira C, Magalhaes J, Costa IS, Aragao A, Neto AG, Martins F, Tavora F. Expression of EGFR and Molecules Downstream to PI3K/Akt, Raf-1-MEK-1-MAP (Erk1/2), and JAK (STAT3) Pathways in Invasive Lung Adenocarcinomas Resected at a Single Institution. Anal Cell Pathol (Amst). 2014; 2014: 352925. https://doi.org/10.1155/2014/352925.

23. Zhang W, Fang Y, Shi X, Zhang M, Wang X, Tan Y. Effect of bisphenol A on the EGFR-STAT3 pathway in MCF-7 breast cancer cells. Mol Med Rep. 2012; 5: 41-7. https://doi.org/10.3892/mmr.2011.583.

24. Denoyelle C, Lambert B, Meryet-Figuiere M, Vigneron N, Brotin E, Lecerf C, Abeilard E, Giffard F, Louis MH, Gauduchon P, Juin P, Poulain L. miR-491-5p-induced apoptosis in ovarian carcinoma depends on the direct inhibition of both BCL-XL and EGFR leading to BIM activation. Cell Death Dis. 2014; 5: e1445. https://doi.org/10.1038/cddis.2014.389.

25. Tokar EJ, Diwan BA, Waalkes MP. Arsenic exposure transforms human epithelial stem/progenitor cells into a cancer stem-like phenotype. Environ Health Perspect. 2010; 118: 108-15. https://doi.org/10.1289/ehp.0901059.

26. Jemal A, Bray F, Center MM, Ferlay J, Ward E, Forman D. Global cancer statistics. CA Cancer J Clin. 2011; 61: 69-90. https://doi.org/10.3322/caac.20107.

27. Ferlay J, Shin HR, Bray F, Forman D, Mathers C, Parkin DM. Estimates of worldwide burden of cancer in 2008: GLOBOCAN 2008. Int J Cancer. 2010; 127: 2893-917. https://doi.org/10.1002/ijc.25516.

28. Li LM, Hu ZB, Zhou ZX, Chen X, Liu FY, Zhang JF, Shen HB, Zhang CY, Zen K. Serum microRNA profiles serve as novel biomarkers for HBV infection and diagnosis of HBV-positive hepatocarcinoma. Cancer Res. 2010; 70: 9798-807. https://doi.org/10.1158/0008-5472.CAN-10-1001.

29. Zhu C, Ren C, Han J, Ding Y, Du J, Dai N, Dai J, Ma H, Hu Z, Shen H, Xu Y, Jin G. A five-microRNA panel in plasma was identified as potential biomarker for early detection of gastric cancer. Br J Cancer. 2014; 110: 2291-9. https://doi.org/10.1038/bjc.2014.119.

30. Zhou Y, Li Y, Ye J, Jiang R, Yan H, Yang X, Liu Q, Zhang J. MicroRNA-491 is involved in metastasis of hepatocellular carcinoma by inhibitions of matrix metalloproteinase and epithelial to mesenchymal transition. Liver Int. 2013; 33: 1271-80. https://doi.org/10.1111/liv.12190.

31. Li BS, Zhao YL, Guo G, Li W, Zhu ED, Luo X, Mao XH, Zou QM, Yu PW, Zuo QF, Li N, Tang B, Liu KY, et al. Plasma microRNAs, miR-223, miR-21 and miR-218, as novel potential biomarkers for gastric cancer detection. PLoS One. 2012; 7: e41629. https://doi.org/10.1371/journal.pone.0041629.

32. Guo R, Wang Y, Shi WY, Liu B, Hou SQ, Liu L. MicroRNA miR-491-5p targeting both TP53 and Bcl-XL induces cell apoptosis in SW1990 pancreatic cancer cells through mitochondria mediated pathway. Molecules. 2012; 17: 14733-47. https://doi.org/10.3390/molecules171214733.

33. Liang WC, Fu WM, Wong CW, Wang Y, Wang WM, Hu GX, Zhang L, Xiao LJ, Wan DC, Zhang JF, Waye MM. The lncRNA H19 promotes epithelial to mesenchymal transition by functioning as miRNA sponges in colorectal cancer. Oncotarget. 2015; 6: 22513-25. https://doi.org/10.18632/oncotarget.4154.

34. Zhang L, Zhou Y, Huang T, Cheng AS, Yu J, Kang W, To KF. The Interplay of LncRNA-H19 and Its Binding Partners in Physiological Process and Gastric Carcinogenesis. Int J Mol Sci. 2017; 18. https://doi.org/10.3390/ijms18020450.

35. Nicholson RI, Gee JM, Harper ME. EGFR and cancer prognosis. Eur J Cancer. 2001; 37: S9-15.

36. Hoey T, Schindler U. STAT structure and function in signaling. Curr Opin Genet Dev. 1998; 8: 582-7.

37. Nakano H, Miyazawa T, Kinoshita K, Yamada Y, Yoshida T. Functional screening identifies a microRNA, miR-491 that induces apoptosis by targeting Bcl-X(L) in colorectal cancer cells. Int J Cancer. 2010; 127: 1072-80. https://doi.org/10.1002/ijc.25143.

38. Huang WC, Chan SH, Jang TH, Chang JW, Ko YC, Yen TC, Chiang SL, Chiang WF, Shieh TY, Liao CT, Juang JL, Wang HC, Cheng AJ, et al. miRNA-491-5p and GIT1 serve as modulators and biomarkers for oral squamous cell carcinoma invasion and metastasis. Cancer Res. 2014; 74: 751-64. https://doi.org/10.1158/0008-5472.CAN-13-1297.

39. Hrdlickova R, Nehyba J, Bargmann W, Bose HR, Jr. Multiple tumor suppressor microRNAs regulate telomerase and TCF7, an important transcriptional regulator of the Wnt pathway. PLoS One. 2014; 9: e86990. https://doi.org/10.1371/journal.pone.0086990.

40. Arasada RR, Amann JM, Rahman MA, Huppert SS, Carbone DP. EGFR blockade enriches for lung cancer stem-like cells through Notch3-dependent signaling. Cancer Res. 2014; 74: 5572-84. https://doi.org/10.1158/0008-5472.CAN-13-3724.

41. Sherry MM, Reeves A, Wu JK, Cochran BH. STAT3 is required for proliferation and maintenance of multipotency in glioblastoma stem cells. Stem Cells. 2009; 27: 2383-92. https://doi.org/10.1002/stem.185.

42. Guryanova OA, Wu Q, Cheng L, Lathia JD, Huang Z, Yang J, MacSwords J, Eyler CE, McLendon RE, Heddleston JM, Shou W, Hambardzumyan D, Lee J, et al. Nonreceptor tyrosine kinase BMX maintains self-renewal and tumorigenic potential of glioblastoma stem cells by activating STAT3. Cancer Cell. 2011; 19: 498-511. https://doi.org/10.1016/j.ccr.2011.03.004.

43. Kim SY, Kang JW, Song X, Kim BK, Yoo YD, Kwon YT, Lee YJ. Role of the IL-6-JAK1-STAT3-Oct-4 pathway in the conversion of non-stem cancer cells into cancer stem-like cells. Cell Signal. 2013; 25: 961-9. https://doi.org/10.1016/j.cellsig.2013.01.007.

44. Thiagarajan PS, Zheng Q, Bhagrath M, Mulkearns-Hubert EE, Myers MG, Lathia JD, Reizes O. STAT3 activation by leptin receptor is essential for TNBC stem cell maintenance. Endocr Relat Cancer. 2017; 24: 415-26. https://doi.org/10.1530/ERC-16-0349.

45. Shen YA, Wang CY, Chuang HY, Hwang JJ, Chi WH, Shu CH, Ho CY, Li WY, Chen YJ. CD44 and CD24 coordinate the reprogramming of nasopharyngeal carcinoma cells towards a cancer stem cell phenotype through STAT3 activation. Oncotarget. 2016; 7: 58351-66. https://doi.org/10.18632/oncotarget.11113.

46. Lin CY, Tsai PH, Kandaswami CC, Lee PP, Huang CJ, Hwang JJ, Lee MT. Matrix metalloproteinase-9 cooperates with transcription factor Snail to induce epithelial-mesenchymal transition. Cancer Sci. 2011; 102: 815-27. https://doi.org/10.1111/j.1349-7006.2011.01861.x.

47. Han M, Liu M, Wang Y, Mo Z, Bi X, Liu Z, Fan Y, Chen X, Wu C. Re-expression of miR-21 contributes to migration and invasion by inducing epithelial-mesenchymal transition consistent with cancer stem cell characteristics in MCF-7 cells. Mol Cell Biochem. 2012; 363: 427-36. https://doi.org/10.1007/s11010-011-1195-5.

48. Yan W, Zhang W, Sun L, Liu Y, You G, Wang Y, Kang C, You Y, Jiang T. Identification of MMP-9 specific microRNA expression profile as potential targets of anti-invasion therapy in glioblastoma multiforme. Brain Res. 2011; 1411: 108-15. https://doi.org/10.1016/j.brainres.2011.07.002.

49. Xu XM, Yuan GJ, Li QW, Shan SL, Jiang S. Hyperthermia inhibits transforming growth factor beta-induced epithelial-mesenchymal transition (EMT) in HepG2 hepatocellular carcinoma cells. Hepatogastroenterology. 2012; 59: 2059-63. https://doi.org/10.5754/hge12404.

50. Ding SJ, Li Y, Shao XX, Zhou H, Zeng R, Tang ZY, Xia QC. Proteome analysis of hepatocellular carcinoma cell strains, MHCC97-H and MHCC97-L, with different metastasis potentials. Proteomics. 2004; 4: 982-94. https://doi.org/10.1002/pmic.200300653.

51. Xu Y, Li Y, Pang Y, Ling M, Shen L, Yang X, Zhang J, Zhou J, Wang X, Liu Q. EMT and stem cell-like properties associated with HIF-2alpha are involved in arsenite-induced transformation of human bronchial epithelial cells. PLoS One. 2012; 7: e37765. https://doi.org/10.1371/journal.pone.0037765.

52. Luo F, Xu Y, Ling M, Zhao Y, Xu W, Liang X, Jiang R, Wang B, Bian Q, Liu Q. Arsenite evokes IL-6 secretion, autocrine regulation of STAT3 signaling, and miR-21 expression, processes involved in the EMT and malignant transformation of human bronchial epithelial cells. Toxicol Appl Pharmacol. 2013; 273: 27-34. https://doi.org/10.1016/j.taap.2013.08.025.